ACS chemical biology

Articles

pubs.acs.org/acschemicalbiology

RNA Mango Aptamer-Fluorophore: A Bright, High-Affinity Complex for RNA Labeling and Tracking

Elena V. Dolgosheina,[†] Sunny C. Y. Jeng,[†] Shanker Shyam S. Panchapakesan,[†] Razvan Cojocaru,[†] Patrick S. K. Chen,[‡] Peter D. Wilson,[‡] Nancy Hawkins,[†] Paul A. Wiggins,[§] and Peter J. Unrau*,[†]

[†]Department of Molecular Biology and Biochemistry and [‡]Department of Chemistry, Simon Fraser University, 8888 University Road, Burnaby, British Columbia V5A 1S6, Canada

[§]Department of Physics, Bioengineering and Microbiology, University of Washington, 3910 15th Avenue, NE, Seattle, Washington 98195, United States

Supporting Information

ABSTRACT: Because RNA lacks strong intrinsic fluorescence, it has proven challenging to track RNA molecules in real time. To address this problem and to allow the purification of fluorescently tagged RNA complexes, we have selected a high affinity RNA aptamer called RNA Mango. This aptamer binds a series of thiazole orange (fluorophore) derivatives with nanomolar affinity, while increasing fluorophore fluorescence by up to 1,100-fold. Visualization of RNA Mango by single-molecule fluorescence microscopy, together with injection and imaging of RNA Mango/fluorophore complex in *C. elegans* gonads demonstrates the potential for live-cell RNA imaging with this system. By inserting RNA Mango into a stem loop of the bacterial 6S RNA and biotinylating the fluorophore, we demonstrate that the aptamer can be used to simultaneously fluorescently label and purify biologically important RNAs. The high affinity and fluorescent properties of RNA Mango are therefore expected to simplify the study of RNA complexes.

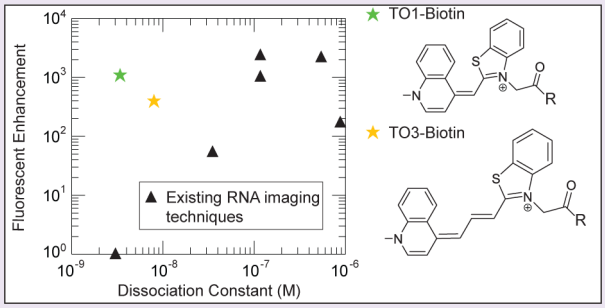

The detection of low abundance RNA *in vitro* or *in vivo* has proven to be difficult, and much effort has been devoted to developing nanostructured fluorescent probes for imaging RNA *in vivo*.[1−5] Because strongly fluorescent RNAs do not exist,[6,7] fluorescent reporter molecules must be recruited to RNA, normally through noncovalent binding to a compatible tag region (e.g., sequence or tertiary structure) incorporated into the RNA target. As such, both the K_D and the fluorescent efficiency (defined here as $E = F_E/K_D$, where F_E is the fluorescent enhancement observed between bound and unbound fluorophore) are important parameters to optimize when tracking RNA in low concentrations.

In an ideal RNA tracking system, K_D should be minimized, as only then will low concentrations of RNA be fully complexed with fluorophore, while E should be maximized, so that the signal-to-noise ratio of the system is as high as possible. Systems, such as the GFP-MS2[8] and the recent Spinach aptamer,[1,9,10] optimize one or the other of these two constraints but fail to simultaneously optimize both (Table 1). The MS2 system fuses a fluorescent protein reporter to a peptide sequence recognized by an RNA motif with nanomolar affinity and has proven successful in RNA live cell imaging.[11−18] Yet, it suffers since the intrinsic fluorescence of the unbound protein reporter is not enhanced upon binding to the target RNA (i.e., $F_E = n$, where n is the number of encoded MS2 RNA sequence elements), making it potentially difficult to discern the signal coming from the free fluorophore itself or the fluorophore bound to RNA. Conversely, despite the high fluorescent enhancement of the Spinach aptamer (F_E = 2,000), the system has a poor K_D.[9] This places the fluorescent efficiency of the Spinach aptamer some six times lower than that of the toxic malachite green aptamer (Table 1), which has both a higher F_E and lower K_D.[19−21]

For single molecule imaging and for the purification of RNA complexes, low K_D, or more specifically a slow off-rate from the RNA fluoromodule, takes on an additional significance: A single bound complex should persist for the duration of imaging and/or complex purification. In this study we present RNA Mango, an RNA aptamer with nanomolar fluoromodule binding affinity comparable to that found in the MS2 system[22] and with fluorescent enhancement similar to that found in the Spinach system[9] (Table 1). In terms of fluorescent efficiency, RNA Mango is nearly 3 orders of magnitude superior to the MS2 system and nearly 2 orders of magnitude superior to the Spinach system. As we demonstrate, the high binding affinity of RNA Mango to its fluorophore makes possible single molecule RNA visualization and offers the potential to fluorescently monitor RNA complexes while simultaneously using the fluorophore as a purification tag.

Received: June 23, 2014
Accepted: August 7, 2014

   dx.doi.org/10.1021/cb500499x | *ACS Chem. Biol.* XXXX, XXX, XXX−XXX

Table 1. RNA Aptamer/Fluoromodule Complex Properties

fluoromodule complex	rel E^a	$F_E{}^b$	$K_D{}^c$ (nM)	ex (nm)	em (nm)	ε^d (M^{-1} cm^{-1})	ϕ^e
GFP-MS2[8]	1	1	~3	395	508	27,600	0.79
Malachite Green[19]	62	2,400	117	630	650	150,000	0.19
RNA Spinach[9]	11−20	2,000	300−540	469	501	24,300	0.72
RNA Mango (TO1-Biotin)	970	1,100	3.2	510	535	77,500	0.14

[a]Fluorescent efficiencies, defined as $E = F_E/K_D$, were normalized to the GFP-MS2 construct assuming only one MS2 RNA binding element ($n = 1$). [b]Fluorescent enhancement of bound complex relative to unbound fluorophore. [c]Dissociation constant for the complex. [d]Extinction coefficient. [e]Fluorescence quantum yield.

RESULTS AND DISCUSSION

TO1-Biotin Fluorophore Synthesis. Thiazole Orange (TO1) is an asymmetric cyanine fluorophore, which contains a benzothiazole ring covalently linked to a quinoline ring via a monomethine bridge. In aqueous solution the fluorophore exhibits very low fluorescence (λ_{ex} = 500 nm, λ_{em} = 525 nm, $\phi = 2 \times 10^{-4}$) due to rapid nonradiative decay through the torsional motion in the monomethine bridge joining the two heterocycles. Normally, TO1 becomes strongly fluorescent when the monomethine bridge connecting the two heterocycles is rigidified through nonspecific insertion into double-stranded helical nucleic acids giving a fluorescence quantum yield of 0.11.[23,24] TO1 fluorophore possesses several characteristics that make it an ideal fluorophore for the selection of an aptamer, which include small size, lack of toxicity, plasma and nuclear membrane permeability,[25,26] short intracellular half-life,[25] and the accessibility of a broad wavelength range via simply synthesized TO1 analogues.[27,28] The main complication with TO1 is its tendency to bind nonspecifically to cellular DNA or RNA at micromolar concentrations, which could potentially cause cellular background fluorescence.

To overcome this limitation, we synthesized TO1-Acetate. This modification has previously been shown to destabilize nucleic acid intercalation[29] and allowed us to attach a biotin tag for *in vitro* selection and subsequent complex purification (Figure 1A, Supplementary Methods). When incubated with random sequence RNA, TO1-Biotin was found to have a fluorescent response that was ~7 times lower than that observed with TO1 (Supplementary Figure S1), confirming that this construct reduced nonspecific interactions with RNA.

***In Vitro* Selection of RNA Mango.** An RNA pool containing ~3×10^{13} distinct sequences was obtained by *in vitro* transcription of the corresponding random sequence DNA pool (see Supporting Information) and was subjected to multiple rounds of high affinity selection. At the beginning of each round, streptavidin magnetic beads were derivatized with TO1-Biotin. Excess fluorophore was washed away, and the previously denatured radiolabeled RNA pool was applied to the beads at 37 °C in a physiologically relevant buffer. After 30 min of incubation bound RNA molecules were eluted using KOH, or a formamide/EDTA solution in later rounds. Recovered RNA was RT-PCR amplified prior to transcription of the next round of RNA pool.

After five rounds of selection the stringency was dramatically increased, so as to encourage the isolation of fast on-rate, slow off-rate fluorophore binders. Binding and incubation times were reduced from 30 to 1 min, while the three wash times were increased from a total time of 3 to 60 min (see Supporting Information). The last two washes were performed using diluted wash buffer, where the ionic strength had been lowered by 10-fold. Equally important, 12 μM of free TO1 was added to all washes so as to aggressively compete for RNA molecules that were able to transiently disassociate from the streptavidin-immobilized TO1-Biotin (see Supporting Information). In total, 12 rounds of selection were performed. The final pool was found to consist only of RNA molecules that had a high affinity for TO1-Biotin-derivatized beads. These RNA molecules had little if any affinity for streptavidin beads alone.

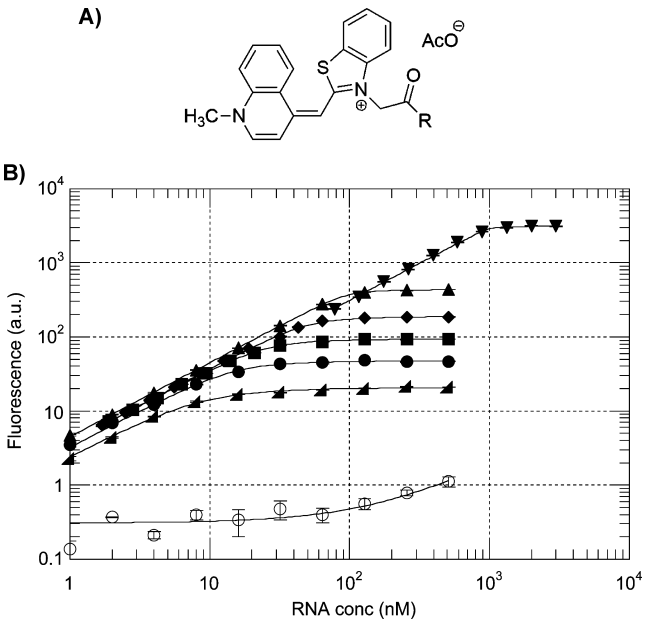

Figure 1. RNA Mango has a high binding affinity to TO1-Biotin. (A) TO1 fluorophore, R = Biotin-PEG_3-amine (compound 6, see Supporting Information) used in selection. (B) RNA Mango aptamer binds to TO1-Biotin over a broad concentration range. Fluorophore concentrations: 5 nM, right triangles; 10 nM, circles; 20 nM, squares; 40 nM, diamonds; 100 nM, triangles; 1000 nM, inverted triangles. The initial unselected pool when incubated with 10 nM TO1-Biotin is shown by open circles. Error bars are standard deviations about the mean of three measurements.

Twenty-four isolates from the final round of selection were sequenced and fell into a total of 7 distinct families (Supplementary Figure S2). Each family was screened for its ability to bind and enhance fluorescence when incubated with TO1-Biotin. While one family had a marginally higher fluorescent response (Family F), the RNA Mango family (Family G) exhibited both tight binding and a high fluorescent enhancement and became the focus of this study.

Characterization of the RNA Mango:TO1-Biotin Complex. The RNA Mango pool isolate binds rapidly to TO1-Biotin with nanomolar affinity (Figure 1B). Fluorescent response fit well to a simple one-to-one aptamer-fluorophore binding model (eq 1) and yielded a K_D of 3.2 ± 0.7 nM. Titrating the initial unselected random sequence pool of RNA (Round 0 RNA) against 10 nM of TO1-Biotin fluorophore

dx.doi.org/10.1021/cb500499x | ACS Chem. Biol. XXXX, XXX, XXX−XXX

resulted in a fluorescent response that was at the limits of detection of the fluorimeter until a RNA concentration of ~100 nM was reached. At this point, a linear fluorescent response was observed (Figure 1B) that was 3 orders of magnitude smaller than the initial slopes for all RNA Mango titrations shown. Consistent with its high binding affinity, fluorescent scans of native gel-shifts of RNA Mango:TO1-Biotin complexes were easily obtained (Supplementary Figure S3), suggesting that the RNA Mango-fluorophore complex has a slow off-rate. On-rates measured using 100 nM RNA Mango and 10 to 40 nM TO1-Biotin were found to occur within 30 s (Figure 2). Such binding

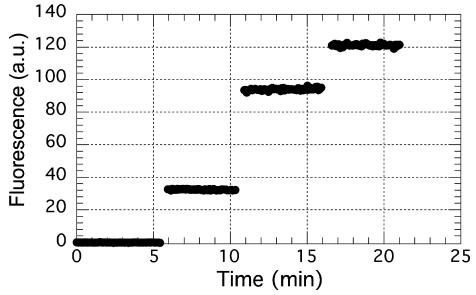

Figure 2. Mango:TO1-Biotin complex formation is rapid. Aliquots of concentrated TO1-Biotin were sequentially added to a cuvette containing 100 nM RNA Mango so as to result in 10, 30, and 40 nM final concentrations of TO1-Biotin. The fluorimeter was paused for 30 s during addition of each fluorophore aliquot.

kinetics and high binding affinity, while not unusual for antibodies,[30,31] is unusual for an RNA aptamer and to our knowledge has been exceeded only by aptamers selected against the glycoside-type antibiotics.[32]

A reselection of RNA Mango was performed to identify its core motif (see Supporting Information). Reselection did not significantly improve binding, suggesting that the RNA Mango motif was already optimal. This hypothesis was validated by the discovery of a highly conserved 23-nt core: 5′-(G/U)**AA *GG* GA**(C/U/A) ***GG* UG**(C/U/A) ***GG* AG**(A/U) ***GG* AGA**, which was common to all highly fluorescent reselected isolates (see Supplementary Figure S2.B). Residues in bold were highly conserved and served to space four absolutely conserved G pairs (bold italics). Isolates that violated this core sequence motif were found to lack fluorescence, strongly suggesting that this motif was responsible for fluorescent response. Immediately on either side of this core sequence, a short closing stem was indicated by covariational analysis (Supplementary Figure S2.B). Constructs closed by four distinct 8-bp stems were found to be sufficient for binding and fluorescent enhancement (Supplementary Figure S4). Removing the closing stem destroyed fluorescence and indicated that a minimal RNA Mango construct could be constructed from as little as 39 nt of sequence.

The pattern of four regularly spaced G pairs is strongly suggestive of a G-quadruplex with 3-nt propeller arms (Figure 3A). Potassium, which is known to stabilize G-quadruplexes much more effectively than other monovalent ions, was found to be essential for fluorescence. When RNA Mango was titrated, much smaller fluorescent enhancements were observed when only sodium was present, and still less fluorescent enhancement was observed with lithium (Figure 3B). Titrating potassium revealed a Hill coefficient of 1.6 ± 0.1, indicating that at least one potassium ion is required for a strong fluorescent response to occur. CD spectra of the potassium fluorophore-bound complex are suggestive of a parallel-stranded G-quadruplex,[33] since a negative rotation in the 220−240 nm region appeared only after the addition of fluorophore in the presence of KCl. This negative rotation was accompanied by a positive rotation in the 260 nm region (Supplementary Figure S5). Consistent with the CD data, native T1 RNase probing experiments indicated that the core G residues become strongly protected only when potassium and TO1-Biotin were present simultaneously (Figure 3C). Taken together these data indicate that a compact, potassium-dependent, parallel-stranded G-quadruplex structure forms upon fluorophore binding.

The proposed RNA Mango quadruplex structure and its fluorophore-binding capabilities were explored further by extending the 2G stack structure by another G-quadruplex layer. This change decreased binding affinity from 3.2 to ~70 nM with a 50% loss in maximum fluorescent enhancement (Supplementary Figure S6). In a parallel-stranded G-quadruplex model, increasing the 2G stack to a 3G stack would be expected to distort the 3-nt propeller arms and could, as a consequence, result in a partial loss in binding affinity and/or total fluorescent enhancement. Since the reselected RNA Mango sequences showed absolute conservation of sequence for the propeller nucleotides that are located 3′ to each G pair (henceforth "top" face) and since the nucleotides at the 5′ ends of each pair were poorly conserved, we hypothesize that the top face of the quadruplex serves as the fluorophore-binding surface (Figure 3A). Consistent with this idea, inserting four adenosine residues immediately 5′ to each 3G sequence, so as to relax strain in the propeller arms, partially rescued the 3G fluorescent defect. Maximal fluorescent response increased from 50% to 80% relative to the original RNA Mango construct (Supplementary Figure S6). That the 3G construct could be partially rescued in such a simple fashion is fully consistent with RNA Mango being a parallel-stranded G-quadruplex structure that binds TO1 fluorophore on the top face of the quadruplex.

Stacking TO1 fluorophore onto the top face of the G-quadruplex structure of RNA Mango immediately suggests a mechanism by which the RNA Mango aptamer prevents free rotation between the benzothiazole and quinoline rings of TO1-Biotin, so as to achieve a highly fluorescent bound state. Further support for quadruplex face binding was provided by the observation of a strong fluorescent excitation at 260 nm (Figure 4A). Notably, this excitation has a long-wavelength shoulder (295 nm) that is reminiscent of the UV absorbance profile of guanine.[34] Such a fluorescent excitation would be expected if TO1 fluorophore is electronically coupled to the G-quartet structure of the quadruplex.

Fluorescent and Binding Properties of RNA Mango with TO1 Derivatives. RNA Mango complexed with TO1-Biotin generated a fluorescent enhancement of 1,100-fold relative to unbound fluorophore with strong excitation peaks observed at both 260 and 510 nm (Figure 4A). Emission was centered at 535 nm. Both the 510 nm excitation and 535 nm emission were red-shifted by ~10 nm with respect to unbound fluorophore (Supplementary Figure S7). The extinction coefficient for the bound complex at 510 nm was determined to be 77,500 M^{-1} cm^{-1}. The quantum yield for fluorescence was 0.14 as judged relative to a fluorescein standard in 0.1 mM NaOH. This value is slightly higher than previously observed for TO1 intercalation into double-stranded DNA, where quantum yields of 0.11 have been reported.[23,35,36] The overall brightness of RNA Mango was found to be ~11,000 M^{-1} cm^{-1},

dx.doi.org/10.1021/cb500499x | ACS Chem. Biol. XXXX, XXX, XXX−XXX

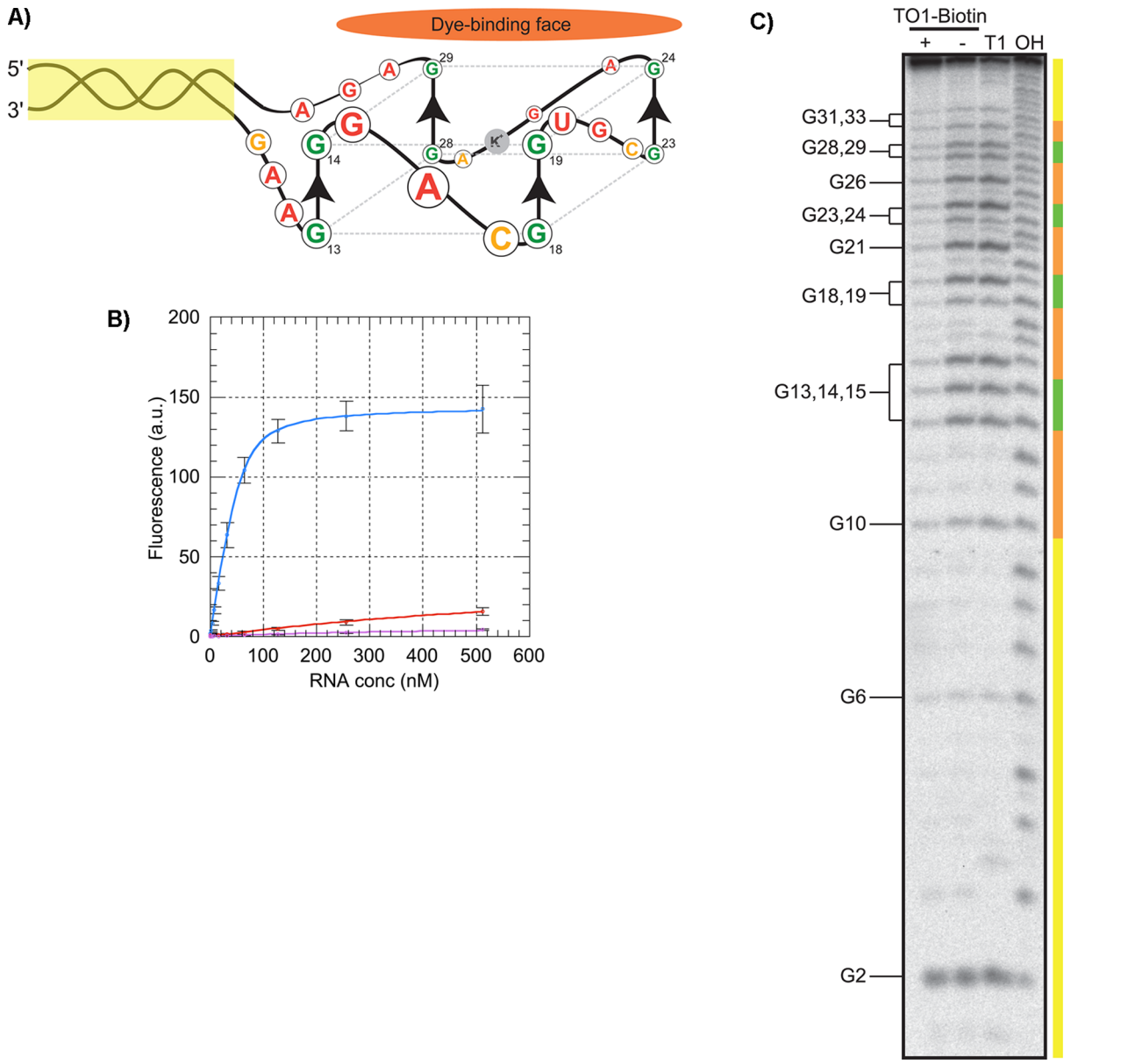

Figure 3. Secondary structure of RNA Mango. (A) Proposed G-quadruplex structure of RNA Mango. Residues in red were highly conserved in functional isolates, while residues in yellow were observed to vary. G-quadruplex residues are shown in green. (B) RNA Mango requires potassium to strongly fluoresce. RNA titrations were performed in a Tris-based buffer (10 mM pH 7.2), containing 50 nM TO1-Biotin and 140 mM concentration of either KCl (blue), NaCl (red), or LiCl (purple). (C) Native T1 RNase protection assay: 5′ radiolabeled RNA Mango (Construct 1, Supplementary Figure S4) was analyzed by native T1 RNase digest with or without addition of TO1-Biotin fluorophore (lane 1 and 2, respectively) and compared to denaturing T1 RNase and alkaline hydrolysis reference lanes (lanes 3 and 4, respectively). Samples were resolved by 20% denaturing PAGE. Color coding: yellow, stem region; green, G residues in quadruplex; orange, propeller regions of proposed quadruplex.

implying that three repeats of RNA Mango should generate fluorescence with intensity comparable to enhanced green fluorescent protein (brightness of 34,000 M^{-1} cm^{-1}).[37]

A series of TO1 derivatives were synthesized and tested for their binding and fluorescent enhancement properties. TO1 and TO1-Acetate were found not to strongly fluoresce when added to RNA Mango, suggesting that elements of the linker between TO1 and biotin play an important role in either binding or fluorescent enhancement. Biotin was found not to be essential for binding, and a series of constructs with fluorescent enhancements comparable to RNA Mango:TO1-Biotin were easily found. A three-carbon alkane spacer together with a methoxyethane derivative both showed a 2-fold decrease in binding affinity and a 5-fold decrease in fluorescent enhancement (compounds 1 and 2, Supplementary Table S2), while two PEG derivatives each terminated with an alkylated amide (compounds 3 and 4, Supplementary Table S2) bound with an affinity indistinguishable from that of TO1-Biotin and exhibited only a 2- to 3-fold loss in fluorescent enhancement. We hypothesize that if the TO1 fluorophore is stacked onto the top face of the RNA Mango G-quadruplex, then the fluorophore side chain may be interacting hydrophobically with unpaired nucleotides found in the 3-nt propeller arms of the quadruplex (Figure 3A). Consistent with this hypothesis, compound 7 (Supplementary Table S2), which has a 2-carbon alkane spacer, showed decreased binding, while compound 8 (Supplementary Table S2), which has a 5-carbon alkane spacer, exhibited enhanced binding and

dx.doi.org/10.1021/cb500499x | ACS Chem. Biol. XXXX, XXX, XXX–XXX

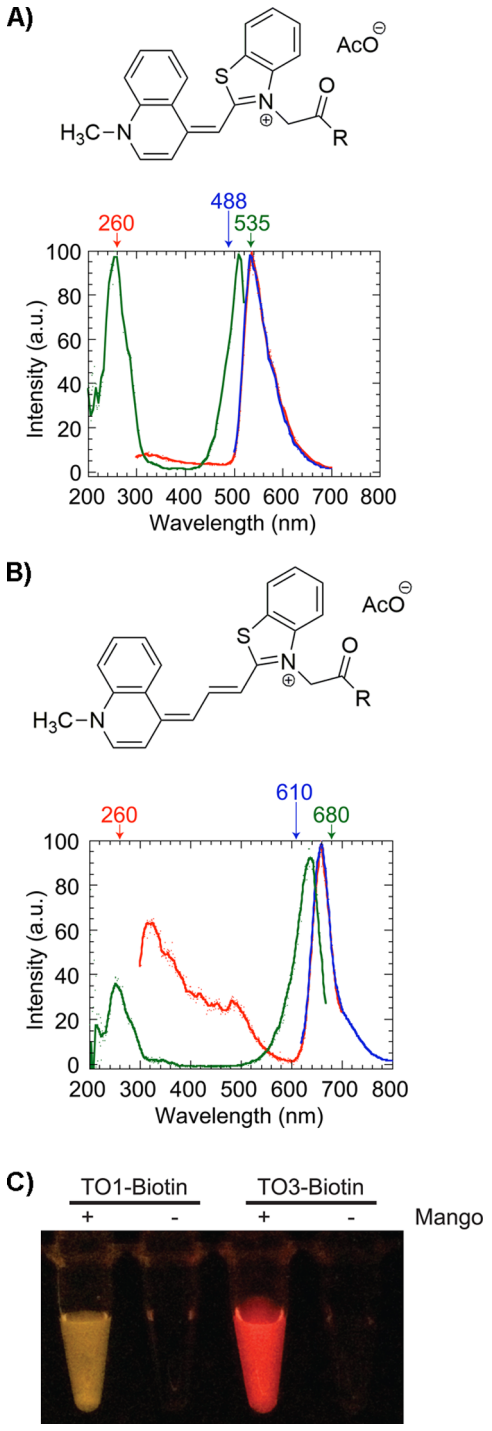

Figure 4. Fluorescent properties of the RNA Mango complex. (A, B) Excitation and emission scans were performed with TO1 or TO3 fluorophores (40 nM) bound to an excess of RNA Mango. Excitation wavelengths are indicated in red and blue, with emission wavelengths being indicated in green. (C) Direct visualization of the RNA Mango:TO1-Biotin or TO3-Biotin complexes using a hand-held short wavelength UV lamp and 2 μM concentration of either fluorophore.

undiminished fluorescent enhancement. Compound 9, which adds a pyrazine group to TO1, provides some additional support for our hypothesis, as this derivative binds with high affinity and exhibits only a 4-fold loss in fluorescent enhancement. Further characterization of the RNA Mango-fluorophore interaction appears likely to require detailed information from NMR or X-ray crystallography.

Fluorescent and Binding Properties of RNA Mango to TO3-Biotin. If TO1 derivatives bind to RNA Mango with nanomolar affinity, is it possible that our aptamer can induce fluorescence with other thiazole orange derivatives? Such fluorophores are of particular interest if they allow fluorescent imaging further into the infrared region, where biologically derived fluorescence background is greatly attenuated.[38] To explore this possibility, we synthesized TO3-Biotin (see Supporting Information), which is significantly red-shifted with respect to the TO1 fluorophore. RNA Mango:TO3-Biotin complex (Figure 4B) has an excitation at 637 nm that is fully compatible with standard solid state 640 nm red lasers. Emission was found to be maximal at 658 nm, 10 nm beyond that of the far-red fluorescent protein mPlum.[37] Just as for TO1-Biotin, excitation at 260 nm was observed together with a high wavelength shoulder (295 nm) resembling the absorbance spectrum of guanine. This suggests that, upon binding, TO3 fluorophore is also electronically coupled to the guanine face of the G-quadruplex found in RNA Mango. The extinction coefficient of TO3-Acetate was found to be 9,300 M^{-1} cm^{-1}, considerably lower than that observed for TO1-Biotin. Nevertheless, a short wavelength UV hand-held lamp readily generated fluorescence from both 2 μM RNA Mango:TO1-Biotin complex and 2 μM RNA Mango:TO3-Biotin complex (Figure 4C).

When TO3-Biotin concentrations were lower than 50 nM, a one-to-one binding model fit well to data and suggested a K_D of 6−8 nM. At higher fluorophore concentrations, an enhancement in fluorescence at low RNA concentrations was observed that steadily diverged from the expected one-to-one binding model as fluorophore concentrations were increased (Supplementary Figure S8). The source of this fluorophore-dependent effect has not been determined but may be related to the propensity of the TO3 fluorophore to dimerize at micromolar concentrations.

Single Molecule Imaging. In order to visualize single molecule complexes of RNA Mango and TO1-Biotin, fluorophore was mixed with an excess of streptavidin and immobilized on glass slide flow cells (see Supplementary Methods) and imaged by TIRF until photobleaching occurred. A representative image sequence is shown in Figure 5. The RNA Mango complex was found to be 0.3 ± 0.1 times as bright as a yPet control, which has a brightness free in solution of 80,000 M^{-1} cm^{-1}.[37,39] This 2-fold enhancement in fluorescence relative to the previously calculated brightness for RNA Mango complex free in solution may not be significant, but we note a comparable increase in fluorescent signal in our gel-shift results upon addition of streptavidin (Supplementary Figure S3). This suggests the possibility that further enhancements in quantum yield of the RNA Mango-TO1-Biotin complex will be possible in the future.

RNA Mango *in Vivo*: Injection into *C. elegans* and Bacterial Expression. To explore the potential of RNA Mango for the direct visualization of cellular RNAs, we deliberately injected 100 μM TO1-Biotin into *C. elegans* syncytial gonads, either with or without equimolar amounts of RNA Mango (Construct 1, Supplementary Figure S4). While injection of dye alone resulted in negligible fluorescence, injection of RNA Mango:TO1-Biotin complex resulted in a strong signal (Supplementary Figure S9). At longer exposures, where RNA Mango-fluorophore complex signal was saturated,

dx.doi.org/10.1021/cb500499x | ACS Chem. Biol. XXXX, XXX, XXX−XXX

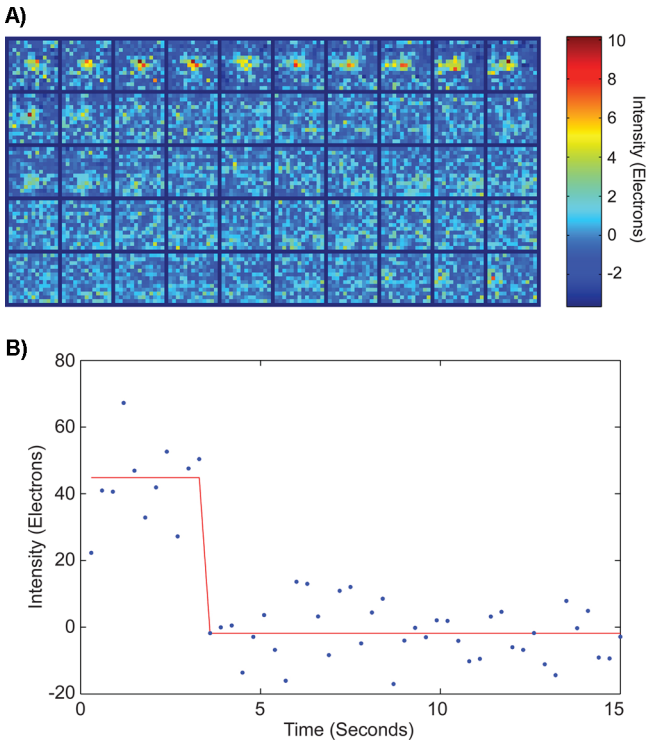

Figure 5. Single molecule detection of RNA Mango complex with TO1-Biotin. (A) A typical image series showing the photobleaching of a single RNA Mango-TO1-Biotin complex. (B) For each image series, the focus intensity was computed to plot an intensity trace.

only a faint TO1-Biotin signal was observed at the site of injection (Supplementary Figure S9.D) indicating that TO1-Biotin does not significantly fluoresce with the biological material found in a worm gonad. Interestingly, the RNA Mango-fluorophore complex preferentially and rapidly (<10 min) localized to the syncytial nuclei of the gonad. The source of this localization is unknown. Observing staged worms over a period of 2 h postinjection demonstrated that not only was the RNA Mango-fluorophore complex bright *in vivo*, but that the fluorescence was substantially undiminished within this time frame.

Gram-negative bacteria such as *E. coli* present a potent test for cell permeability. We therefore investigated whether or not the RNA Mango fluoromodule could be detected in BL21 (DE3) *E. coli* cells transformed with a plasmid able to overexpress RNA Mango (Supplementary Figure S10.A). At 1.5 h prior to performing FACS (Millipore Guava, 488 nm laser, emission filter 525/530), 5 μM TO1-Biotin was added to the growth medium of induced and uninduced cells. An increase in cellular fluorescence was observed that was conditional on IPTG-based induction of RNA Mango (Supplementary Figure S10.B). Similar experiments with RNA Spinach report a 200 μM concentration of fluorophore being required to detect bacterial fluorescence.[9] Assuming that the cellular concentrations of both fluorophores are in proportion to the external fluorophore concentration, then the nearly 2 orders of magnitude difference in fluorophore concentration required between RNA Mango and RNA Spinach may largely be attributable to the 100-fold difference in binding affinity between the two aptamers (Table 1).

Integration of RNA Mango into the Bacterial 6S Transcriptional Control RNA. Many biological RNAs contain stem loops that are not essential for function. For example, the 6S transcriptional control RNA, which binds and releases from bacterial RNA polymerase (H.E.) via an NTP-dependent mechanism,[40,41] has a nonconserved stem loop structure[42] (Figure 6A). We replaced this loop sequence with RNA Mango (Figure 6B) and found that, *in vitro*, the construct allowed the RNA Mango-dependent monitoring of 6S RNA binding and release. The properties of the RNA Mango-tagged 6S was indistinguishable from untagged 6S RNA as monitored by radiolabeling both constructs (Figure 6C). The robustness of this binding interaction was further reinforced by capturing the RNA Mango tagged 6S RNA construct onto streptavidin beads using TO1-Biotin as a handle. After three washes with WB, 87% of the construct remained bound to beads, while unmodified 6S RNA binding could not be detected as judged by liquid scintillation counting. As a final demonstration we overexpressed the RNA Mango tagged 6S RNA in *E. coli* and cleanly purified the expressed construct away from total RNA extract (Figure 6D). Together these experiments strongly suggest that RNA Mango can be used to simultaneously track and purify RNA complexes via its high affinity binding to TO1-Biotin.

This work has identified an RNA sequence optimally selected to bind TO1 type fluorophores. The converse strategy is to synthesize fluorophores with high affinity to G-quadruplexes.[43,44] While this synthetic strategy has been remarkably successful, RNA Mango stresses the critical importance of nucleic acid sequence in maximizing overall fluorophore binding affinity and fluorescent enhancement. Previously, TO1 has been used to recognize DNA quadruplex structures, and while F_E values of 100−1000 have been reported, disassociation constants are in 300−3000 nM range.[45] Other promising fluorophores, such as (diisopropyl-guanidino) zinc phthalocyanine (Zn-DIGP) or carbazole derivative BMVC, bind to DNA quadruplexes with nanomolar affinities but have fluorescent enhancements approximately 1−2 orders of magnitude lower than that observed with RNA Mango and TO1-Biotin.[46−48] Potentially, sequences able to bind these or similar fluorophores might be found by *in vitro* selection, but for the time being, RNA Mango and the cyanine TO1 and TO3 fluorophores represent a new standard in the fluorophore-based recognition of a specific RNA G-quadruplex motif.

RNA Mango offers significantly higher fluorescent efficiency than either RNA Spinach or the MS2 systems (Table 1). The small size and simple closing stem structure of RNA Mango indicates that it will be straightforward to incorporate this aptamer into arbitrary biological RNAs without disrupting biological function, as we have demonstrated here using the 6S RNA as an example. The stability of RNA Mango within *C. elegans* gonads and the established permeability of TO1 fluorophores into cells[25] and bacteria (Supplementary Figure S8), together with the very low intrinsic fluorescence of unbound TO1 fluorophores, suggest the potential for RNA Mango to track the spatial and temporal expression of low copy number RNAs within living organisms. Perhaps equally important, the robust binding interaction between RNA Mango and its fluorophore provides a means to not only visualize RNA complexes but to also purify such constructs using a single small RNA aptamer tag.

METHODS

Fluorophore Synthesis and *in Vitro* Selection. TO1 and TO3 fluorophore synthesis was adapted from Carreon et al. and Ikeda et

dx.doi.org/10.1021/cb500499x | *ACS Chem. Biol.* XXXX, XXX, XXX−XXX

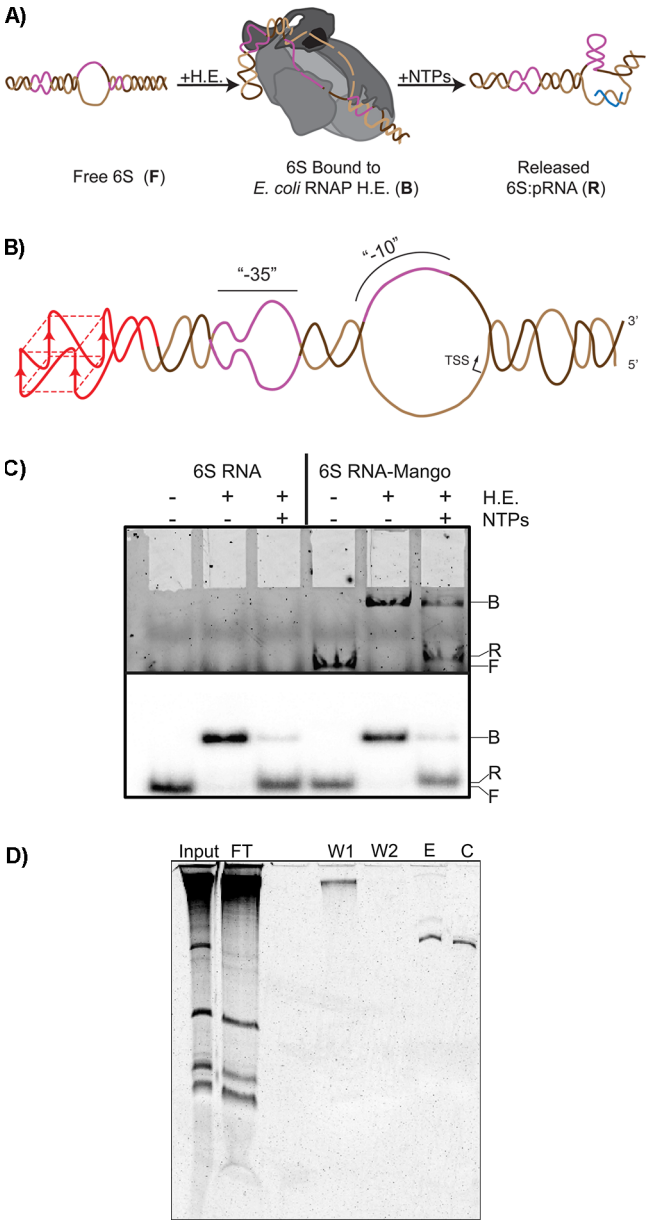

Figure 6. RNA Mango allows monitoring of 6S:holoenzyme complex formation and purification of 6S RNA from total RNA. (A) The 6S RNA has been associated with three states corresponding to unbound 6S RNA (**F**), 6S RNA bound to *E. coli* holoenzyme (**B**), and 6S RNA:pRNA released from holoenzyme by addition of NTPs (**R**). (B) RNA Mango (red) replaced the 5-nt stem loop found in the 6S RNA. The "-35" binding and "-10" regions correspond to highly conserved sequence within the 6S RNA and are shown in purple. (C) Radiolabeled 6S RNA and 6S RNA Mango were prepared in the **F**, **B**, and **R** states and found to behave identically in a native gel assay (phosphorimager scan, bottom panel). RNA Mango fluorescence was captured by a Typhoon imager (488 nm excitation laser, PMT at 600 V, 526 SP filter, top panel). (D) Overexpressed 6S RNA Mango could be purified from bacterial total RNA (Input), using streptavidin beads loaded with TO1-Biotin. E, RNA eluted from beads. C, *in vitro* 6S RNA Mango reference.

al.[35,49] (see Supporting Information). The initial round of selection was performed using 20 nmol of RNA pool having a final sequence of 5′-GGA ACC CGC AAG CCA UC N_{60} GGC UGU GUG AGA UUC UG (N, random nucleotide position), which was synthesized as described in the Supporting Information. Dynabeads M-270 streptavidin (Life Technologies) were complexed with an excess of TO1-Biotin. After unbound fluorophore was washed away, the beads were mixed with heat-denatured pool RNA and incubated for 30 min in wash/binding buffer (WB, 10 mM sodium phosphate pH 7.2, 140 mM KCl, 1 mM $MgCl_2$, and 0.05% Tween-20, RNA pool concentration 4 μM) at 37 °C. After increasingly stringent wash steps (see Supporting Information), bound RNA was recovered and subjected to RT-PCR for the next round of selection.[50] Reselection was performed as described in the Supporting Information.

Binding Affinity and Fluorescent Enhancement Determination. Fluorescent titrations in WB buffer were used to determine dissociation constants. Curves were determined using a nonlinear regression analysis (Kaleidograph) and fitted by least-squares to the following equation:

$$F([\text{apt}]) = F'[(K_D + [\text{apt}] + [\text{fluorophore}]) - \sqrt{(([\text{apt}] - [\text{fluorophore}])^2 + K_D(K_D + 2[\text{apt}] + 2[\text{fluorophore}]))}]/2 \quad (1)$$

where [apt] and [fluorophore] are the RNA aptamer and initial fluorophore concentrations, respectively, and F' is the molar maximum fluorescence (i.e., $F' = F_{max}/[\text{fluorophore}]$). Data was gathered using a Varian Cary Eclipse Fluorescence Spectrophotometer.

Single Molecule Imaging of RNA Mango:TO1-Biotin Complex. TO1-Biotin was immobilized on glass flow-chamber slides, as described in detail in the Supplementary Methods. After the slides were washed, RNA Mango was flowed into the chamber, and the slide was sealed for imaging. Fluorescence excitation was generated by a 514 nm Coherent Sapphire Laser. Beam intensity was estimated to be 1.2 × 10^{-1} $\mu W/\mu m^2$ at the sample. Photons were collected with a Nikon 100X CFI Plan Apo DIC VC 1.4 NA objective, paired with a 150 mm tube lens, and imaged onto an Andor iXon3 897 EMCCD camera.

Integration of RNA Mango into Bacterial 6S RNA. Loop nucleotides 94–98 (sequence 5′-UCCGU) were removed from the *E. coli* 6S RNA and replaced with the core of RNA Mango: 5′-*UAC* GAA **GG** GAC **GG** UGC **GG** AGA **GG** AGA *GUA* together with three additional base pairs of closing stem (in italics). Binding and release assays were performed as described elsewhere using 25 nM RNA,[41] but with the addition of 250 nM TO1-Biotin. 6S RNA construct release was performed for 15 min, after the addition of NTPs and 4 mM $MgCl_2$ and stopped on ice after the addition of an equivolume of loading dye (50% glycerol, 30 mM HEPES pH 7.5, and 180 mM KCl). Samples were analyzed by 5% native PAGE, supplementing the gel with 0.5% glycerol. The gel was made and run using 15 mM HEPES pH 7.5, and 90 mM KCl at 4 °C.

A plasmid carrying the 6S RNA Mango construct was constructed as described in the Supplementary Methods and used to express 6S RNA Mango *in vivo*. A 100 pmol portion of TO1-Biotin was added to 25 μL of Dynabeads M-270 streptavidin that was prepared as for *in vitro* selection. Total RNA (5 μg) was supplemented with 100 μg/mL heparin, 15 mM HEPES pH 7.5, and 90 mM KCl and added to the dye-bound beads. After two washes in 15 mM HEPES pH 7.5 and 90 mM KCl, the bound 6S RNA Mango was recovered in 100 μL of 98% formamide and 10 mM EDTA after a 10 min incubation on a rotator, and 1/10th of the feed, flow through, washes, and eluted RNA were analyzed via 8% denaturing PAGE. The gel was stained with 1X SYBR-Green (Invitrogen) and imaged using an UV trans-illuminator.

■ ASSOCIATED CONTENT

Ⓢ Supporting Information

Detailed chemical synthesis of TO1 derivatives, *in vitro* selection, and related methods. This material is available free of charge via the Internet at http://pubs.acs.org.

■ AUTHOR INFORMATION

Corresponding Author

*E-mail: punrau@sfu.ca.

Notes

The authors declare no competing financial interest.

dx.doi.org/10.1021/cb500499x | *ACS Chem. Biol.* XXXX, XXX, XXX–XXX

REFERENCES

(1) Song, W., Strack, R. L., Svensen, N., and Jaffrey, S. R. (2014) Plug-and-Play fluorophores extend the spectral properties of Spinach. *J. Am. Chem. Soc. 136*, 1198−1201.

(2) Urbinati, C. R., and Long, R. M. (2011) Techniques for following the movement of single RNAs in living cells. *Wiley Interdiscip. Rev.: RNA 2*, 601−609.

(3) Tyagi, S. (2009) Imaging intracellular RNA distribution and dynamics in living cells. *Nat. Methods 6*, 331−338.

(4) Boutorine, A. S., Novopashina, D. S., Krasheninina, O. A., Nozeret, K., and Venyaminova, A. G. (2013) Fluorescent probes for nucleic acid visualization in fixed and live cells. *Molecules 18*, 15357−15397.

(5) Armitage, B. A. (2011) Imaging of RNA in live cells. *Curr. Opin. Chem. Biol. 15*, 806−812.

(6) Kwok, C. K., Sherlock, M. E., and Bevilacqua, P. C. (2013) Effect of loop sequence and loop length on the intrinsic fluorescence of G-quadruplexes. *Biochemistry 52*, 3019−3021.

(7) Mendez, M. A., and Szalai, V. A. (2009) Fluorescence of unmodified oligonucleotides: A tool to probe G-quadruplex DNA structure. *Biopolymers 91*, 841−850.

(8) Bertrand, E., Chartrand, P., Schaefer, M., Shenoy, S. M., Singer, R. H., and Long, R. M. (1998) Localization of ASH1 mRNA particles in living yeast. *Mol. Cell 2*, 437−445.

(9) Paige, J. S., Wu, K. Y., and Jaffrey, S. R. (2011) RNA mimics of green fluorescent protein. *Science 333*, 642−646.

(10) Strack, R. L., Disney, M. D., and Jaffrey, S. R. (2013) A superfolding Spinach2 reveals the dynamic nature of trinucleotide repeat-containing RNA. *Nat. Methods 10*, 1219−1224.

(11) Forrest, K. M., and Gavis, E. R. (2003) Live imaging of endogenous RNA reveals a diffusion and entrapment mechanism for nanos mRNA localization in Drosophila. *Curr. Biol. 13*, 1159−1168.

(12) Querido, E., and Chartrand, P. (2008) Using fluorescent proteins to study mRNA trafficking in living cells. *Methods Cell Biol. 85*, 273−292.

(13) Rook, M. S., Lu, M., and Kosik, K. S. (2000) CaMKIIalpha 3′ untranslated region-directed mRNA translocation in living neurons: Visualization by GFP linkage. *J. Neurosci. 20*, 6385−6393.

(14) Weil, T. T., Forrest, K. M., and Gavis, E. R. (2006) Localization of bicoid mRNA in late oocytes is maintained by continual active transport. *Dev. Cell 11*, 251−262.

(15) Zimyanin, V. L., Belaya, K., Pecreaux, J., Gilchrist, M. J., Clark, A., Davis, I., and Johnston, D., St (2008) In vivo imaging of oskar mRNA transport reveals the mechanism of posterior localization. *Cell 134*, 843−853.

(16) Shav-Tal, Y., Darzacq, X., Shenoy, S. M., Fusco, D., Janicki, S. M., Spector, D. L., and Singer, R. H. (2004) Dynamics of single mRNPs in nuclei of living cells. *Science 304*, 1797−1800.

(17) Golding, I., and Cox, E. C. (2004) RNA dynamics in live Escherichia coli cells. *Proc. Natl. Acad. Sci. U.S.A. 101*, 11310−11315.

(18) Haim, L., Zipor, G., Aronov, S., and Gerst, J. E. (2007) A genomic integration method to visualize localization of endogenous mRNAs in living yeast. *Nat. Methods 4*, 409−412.

(19) Babendure, J. R., Adams, S. R., and Tsien, R. Y. (2003) Aptamers switch on fluorescence of triphenylmethane dyes. *J. Am. Chem. Soc. 125*, 14716−14717.

(20) Fessard, V., Godard, T., Huet, S., Mourot, A., and Poul, J. M. (1999) Mutagenicity of malachite green and leucomalachite green in in vitro tests. *J. Appl. Toxicol 19*, 421−430.

(21) Srivastava, S., Sinha, R., and Roy, D. (2004) Toxicological effects of malachite green. *Aquat. Toxicol. 66*, 319−329.

(22) Johansson, H. E., Dertinger, D., LeCuyer, K. A., Behlen, L. S., Greef, C. H., and Uhlenbeck, O. C. (1998) A thermodynamic analysis of the sequence-specific binding of RNA by bacteriophage MS2 coat protein. *Proc. Natl. Acad. Sci. U.S.A. 95*, 9244−9249.

(23) Nygren, J., Svanvik, N., and Kubista, M. (1998) The interactions between the fluorescent dye thiazole orange and DNA. *Biopolymers 46*, 39−51.

(24) Armitage, B. A. (2005) Cyanine dye-DNA interactions: Intercalation, groove binding, and aggregation. *Top. Curr. Chem. 253*, 55−76.

(25) Weston, S. A., and Parish, C. R. (1990) New fluorescent dyes for lymphocyte migration studies - Analysis by flow-cytometry and fluorescence microscopy. *J. Immunol. Methods 133*, 87−97.

(26) Lee, L. G., Chen, C. H., and Chiu, L. A. (1986) Thiazole Orange - a new dye for reticulocyte analysis. *Cytometry 7*, 508−517.

(27) Ishiguro, T., Saitoh, J., Yawata, H., Otsuka, M., Inoue, T., and Sugiura, Y. (1996) Fluorescence detection of specific sequence of nucleic acids by oxazole yellow-linked oligonucleotides. Homogeneous quantitative monitoring of in vitro transcription. *Nucleic Acids Res. 24*, 4992−4997.

(28) Rye, H. S., Yue, S., Wemmer, D. E., Quesada, M. A., Haugland, R. P., Mathies, R. A., and Glazer, A. N. (1992) Stable fluorescent complexes of double-stranded DNA with bis-intercalating asymmetric cyanine dyes: properties and applications. *Nucleic Acids Res. 20*, 2803−2812.

(29) Carreon, J. R., Mahon, K. P., and Kelley, S. O. (2004) Thiazole orange-peptide conjugates: Sensitivity of DNA binding to chemical structure. *Org. Lett. 6*, 517−519.

(30) Boder, E. T., Midelfort, K. S., and Wittrup, K. D. (2000) Directed evolution of antibody fragments with monovalent femtomolar antigen-binding affinity. *Proc. Natl. Acad. Sci. U.S.A. 97*, 10701−10705.

(31) Griffiths, A. D., Williams, S. C., Hartley, O., Tomlinson, I. M., Waterhouse, P., Crosby, W. L., Kontermann, R. E., Jones, P. T., Low, N. M., Allison, T. J., et al. (1994) Isolation of high affinity human antibodies directly from large synthetic repertoires. *EMBO J. 13*, 3245−3260.

(32) Derbyshire, N., White, S. J., Bunka, D. H., Song, L., Stead, S., Tarbin, J., Sharman, M., Zhou, D., and Stockley, P. G. (2012) Toggled RNA aptamers against aminoglycosides allowing facile detection of antibiotics using gold nanoparticle assays. *Anal. Chem. 84*, 6595−6602.

(33) Vorlickova, M., Kejnovska, I., Sagi, J., Renciuk, D., Bednarova, K., Motlova, J., and Kypr, J. (2012) Circular dichroism and guanine quadruplexes. *Methods 57*, 64−75.

(34) Mergny, J. L., Phan, A. T., and Lacroix, L. (1998) Following G-quartet formation by UV-spectroscopy. *FEBS Lett. 435*, 74−78.

(35) Carreon, J. R., Mahon, K. P., and Kelley, S. O. (2003) Thiazole orange-peptide conjugates: Sensitivity of DNA binding to chemical structure. *Org. Lett. 6*, 517−519.

(36) Svanvik, N., Westman, G., Wang, D., and Kubista, M. (2000) Light-up probes: thiazole orange-conjugated peptide nucleic acid for detection of target nucleic acid in homogeneous solution. *Anal. Biochem. 281*, 26−35.

(37) Shaner, N. C., Steinbach, P. A., and Tsien, R. Y. (2005) A guide to choosing fluorescent proteins. *Nat. Methods 2*, 905−909.

(38) Escobedo, J. O., Rusin, O., Lim, S., and Strongin, R. M. (2010) NIR dyes for bioimaging applications. *Curr. Opin Chem. Biol. 14*, 64−70.

(39) Nguyen, A. W., and Daugherty, P. S. (2005) Evolutionary optimization of fluorescent proteins for intracellular FRET. *Nat. Biotechnol. 23*, 355−360.

(40) Panchapakesan, S. S., and Unrau, P. J. (2012) E. coli 6S RNA release from RNA polymerase requires sigma70 ejection by scrunching and is orchestrated by a conserved RNA hairpin. *RNA 18*, 2251−2259.

(41) Wassarman, K. M., and Saecker, R. M. (2006) Synthesis-mediated release of a small RNA inhibitor of RNA polymerase. *Science 314*, 1601−1603.

(42) Barrick, J. E., Sudarsan, N., Weinberg, Z., Ruzzo, W. L., and Breaker, R. R. (2005) 6S RNA is a widespread regulator of eubacterial RNA polymerase that resembles an open promoter. *RNA 11*, 774−784.

(43) Tarsounas, M., and Tijsterman, M. (2013) Genomes and G-quadruplexes: for better or for worse. *J. Mol. Biol. 425*, 4782−4789.

(44) Bugaut, A., and Balasubramanian, S. (2012) 5′-UTR RNA G-quadruplexes: translation regulation and targeting. *Nucleic Acids Res. 40*, 4727−4741.

(45) Lubitz, I., Zikich, D., and Kotlyar, A. (2010) Specific high-affinity binding of thiazole orange to triplex and G-quadruplex DNA. *Biochemistry 49*, 3567−3574.
(46) Vummidi, B. R., Alzeer, J., and Luedtke, N. W. (2013) Fluorescent probes for G-quadruplex structures. *ChemBioChem 14*, 540−558.
(47) Opresko, P. L., Mason, P. A., Podell, E. R., Lei, M., Hickson, I. D., Cech, T. R., and Bohr, V. A. (2005) POT1 stimulates RecQ helicases WRN and BLM to unwind telomeric DNA substrates. *J. Biol. Chem. 280*, 32069−32080.
(48) Cahoon, L. A., and Seifert, H. S. (2009) An alternative DNA structure is necessary for pilin antigenic variation in Neisseria gonorrhoeae. *Science 325*, 764−767.
(49) Ikeda, S., Kubota, T., Yuki, M., and Okamoto, A. (2009) Exciton-controlled hybridization-sensitive fluorescent probes: multicolor detection of nucleic acids. *Angew. Chem., Int. Ed. 48*, 6480−6484.
(50) Zaher, H. S., and Unrau, P. J. (2005) Nucleic acid library construction using synthetic DNA constructs. *Methods Mol. Biol. 288*, 359−378.